Anal. Chem. **2005,** *77,* 6843−6851

Microfluidic Biosensor Based on an Array of Hydrogel-Entrapped Enzymes

Jinseok Heo and Richard M. Crooks*,†

Department of Chemistry, Texas A&M University, P.O. Box 30012, College Station, Texas 77842-3012

Here we show that a microfluidic sensor based on an array of hydrogel-entrapped enzymes can be used to simultaneously detect different concentrations of the same analyte (glucose) or multiple analytes (glucose and galactose) in real time. The concentration of paraoxon, an acetylcholine esterase inhibitor, can be quantified using the same approach. The hydrogel micropatch arrays and the microfluidic systems are easy to fabricate, and the hydrogels provide a convenient, biocompatible matrix for the enzymes. Isolation of the micropatches within different microfluidic channels eliminates the possibility of cross talk between enzymes.

In this paper, we describe a microfluidic biosensor that uses an array of hydrogel-entrapped enzymes to quantitatively determine the concentration of an analyte and simultaneously detect multiple analytes. The approach relies on the presence of active enzymes within hydrogel micropatches photolithographically defined within microfluidic channels. The enzymes are sufficiently large that they are unable to escape the hydrogel matrix, but the targets are small enough to enter the hydrogel, encounter the enzyme, and be converted into detectable products. By using discrete micropatches contained within multiple channels, and in some cases multiple enzymes within a single hydrogel micropatch, it is possible to detect multiple, structurally similar analytes in parallel and in real time. The apparatus necessary to carry out the assay is straightforward to fabricate.[1−3]

The performance of biosensors incorporating capture probes is directly linked to the approach used for probe immobilization. In this regard, the following issues are important: (1) the biomaterial must remain active on or within the support, (2) nonspecific adsorption should be minimized, (3) the number of probe receptors should be optimized to provide maximum signal, (4) it should be easy to place the immobilized probes in a desired location, and (5) mass transfer of the target from solution to the probe should be rapid. To address these points, we have focused our recent studies on two families of biomolecular supports that are particularly adaptable to the microfluidic environment: polymeric microbeads[4−6] and monolithic hydrogels.[3,7] For example, we reported that photopolymerized hydrogel micropatches could be used for immobilizing enzymes[3] and bacteria[7] within the channels of microfluidic devices. These relatively large biomaterials are physically entrapped within the photo-cross-linked hydrogel matrix, but analytes are able to diffuse through nanopores within the gel and encounter the probes. Importantly, both enzymes and bacteria retain their activity within the gel, which means that the composite gel/biomaterial can be used as a sensor unit or microbioreactor. Here, we expand upon our earlier findings by demonstrating that an array of hydrogel-entrapped enzymes can be used to simultaneously detect multiple analytes or quantitatively determine the concentration of a single analyte.

In addition to our own work, others have shown that hydrogels can be used to immobilize proteins,[8,9] cells,[10−12] and DNA [13−15] within microfluidic devices and on planar supports. The size and shape of the gel can be defined by photolithography,[16,17] a mold,[3,10,12] or a robotic spotter.[18] The smallest hydrogel features reported are in the range of tens of micrometers.[16] Unlike array sensors that rely on surface immobilization of DNA or protein monolayers, which are usually designed to bind specific targets, hydrogel micropatches containing enzymes are essentially microbioreactors that consume reactants and generate products. It is important, therefore, to minimize cross-talk between elements of the array. This issue has been addressed by several groups. For example, Arenkov and co-workers fabricated gel pads on hydrophobic surfaces that were covalently linked to enzymes. The hydrophobic surface prevented sample droplets from spreading to nearby gel pads.[8] McDevitt and co-workers developed an

* To whom correspondence should be addressed. Voice: 979-845-5629. Fax: 979-845-1399. E-mail: crooks@cm.utexas.edu.

† Present address: Department of Chemistry and Biochemistry, The University of Texas, 1 University Station A5300, Austin, TX 78712-0165.

(1) Delamarche, E.; Bernard, A.; Schmid, H.; Michel, B.; Biebuyck, H. *Science* **1997**, *276*, 779−781.
(2) Delamarche, E.; Bernard, A.; Schmid, H.; Bietsch, A.; Michel, B.; Biebuyck, H. *J. Am. Chem. Soc.* **1998**, *120*, 500−508.
(3) Zhan, W.; Seong, G. H.; Crooks, R. M. *Anal. Chem.* **2002**, *74*, 4647−4652.
(4) Seong, G. H.; Crooks, R. M. *J. Am. Chem. Soc.* **2002**, *124*, 13360−13361.
(5) Seong, G. H.; Heo, J.; Crooks, R. M. *Anal. Chem.* **2003**, *75*, 3161−3167.
(6) Seong, G. H.; Zhan, W.; Crooks, R. M. *Anal. Chem.* **2002**, *74*, 3372−3377.
(7) Heo, J.; Thomas, K. J.; Seong, G. H.; Crooks, R. M. *Anal. Chem.* **2003**, *75*, 22−26.
(8) Arenkov, P.; Kukhtin, A.; Gemmell, A.; Voloshchuk, S.; Chupeeva, V.; Mirzabekov, A. *Anal. Biochem.* **2000**, *278*, 123−131.
(9) Guschin, D.; Yershov, G.; Zaslavsky, A.; Gemmell, A.; Shick, V.; Proudnikov, D.; Arenkov, P.; Mirzabekov, A. *Anal. Biochem.* **1997**, *250*, 203-211.
(10) Koh, W. G.; Itle, L. J.; Pishko, M. V. *Anal. Chem.* **2003**, *75*, 5783−5789.
(11) Koh, W. G.; Revzin, A.; Pishko, M. V. *Langmuir* **2002**, *18*, 2459−2462.
(12) Koh, W. G.; Pishko, M. *Langmuir* **2003**, *19*, 10310−10316.
(13) Zangmeister, R. A.; Tarlov, M. J. *Langmuir* **2003**, *19*, 6901−6904.
(14) Zangmeister, R. A.; Tarlov, M. J. *Anal. Chem.* **2004**, *76*, 3655−3659.
(15) Olsen, K. G.; Ross, D. J.; Tarlov, M. J. *Anal. Chem.* **2002**, *74*, 1436−1441.
(16) Beebe, D. J.; Moore, J. S.; Bauer, J. M.; Yu, Q.; Liu, R. H.; Devadoss, C.; Jo, B.-H. *Nature* **2000**, *404*, 588−590.
(17) Revzin, A.; Russel, R. J.; Yadavalli, V. K.; Koh, W.-G.; Deister, C.; Hile, D. D.; Mellott, M. B.; Pishko, M. V. *Langmuir* **2001**, *17*, 5440−5447.
(18) Yadavalli, V. K.; Koh, W. G.; Lazur, G. J.; Pishko, M. V. *Sens. Actuators, B* **2004**, *97*, 290−297.

10.1021/ac0507993 CCC: $30.25
Published on Web 09/24/2005

analysis chip in which individual beads functionalized with different enzymes were placed within cavities micromachined within a silicon substrate.[19]

Here, we report a method for fabricating microfluidic devices that simultaneously perform enzymatic reactions and give rise to easily detectable products. By localizing the enzymes within hydrogel micropatches and confining the micropatches within different microfluidic channels, cross-talk between enzymes is eliminated, the enzymes are stabilized, and transport of reactants and products to and from the enzyme is controlled. These functions are demonstrated by simultaneous detection of glucose and galactose using three parallel sets of hydrogel-entrapped enzyme microreactors, each of which contains a different set of enzymes that is specific for one or the other analyte. The intragel enzymatic reactions are designed to provide a fluorescent signal when the target analyte is present. This same general array-based approach is used to screen enzyme inhibitors. Specifically, we examined paraoxon inhibition of acetylcholinesterase (AChE). In the absence of paraoxon, a model organophosphate, an enzymatic reaction cascade within the hydrogel micropatch leads to a fluorescence signal. However, fluorescence is attenuated following exposure of the enzymes to paraoxon.

EXPERIMENTAL SECTION

Chemicals. PDMS prepolymer (Sylgard 184) was purchased from the Dow Corning Co. (Midland, MI). Positive photoresist (AZ P4620) and developer solution (AZ 421K) were purchased from Clariant Co. (Somerville, NJ). Poly(ethylene glycol) diacrylate (PEG-DA, MW 575), 2-hydroxy-2-methylpropiophenone (HMPP), glucose, and galactose were obtained from the Aldrich Chemical Co. (Milwaukee, WI). Amplex Red (*N*-acetyl-3,7-dihydroxyphenoxazin-3-one) was purchased from Molecular Probes, Inc. (Eugene, OR). 3-(Trichlorosilyl)propyl methacrylate (TPM) was purchased from Fluka Chemicals (Milwaukee, WI). Resorufin, paraoxon, glucose oxidase (GOx, EC 1.1.3.4, type X-S, 157 units/mg of solid from *Aspergillus niger*), horseradish peroxidase (HRP, EC 1.11.1.7, type VI-A, 987 units/mg of solid from horseradish), acetylcholinesterase (AChE, EC 3.1.1.7, type V-S, 1000 units/mg of solid from electric eel), and choline oxidase (ChOx, EC 1.1.3.17, 16−18 units/mg of solid from *Alcaligenes* species) were purchased from the Sigma Chemical Co. (St. Louis, MO). Galactose oxidase (GaOx, EC 1.1.3.9, 109 units/mg, from *Dactylium dendroides*) was purchased from Worthington (Lakewood, NJ). TRIS buffer solution (pH 7.4, 50 mM) was prepared by dissolving 41.4 mmol of tris(hydroxymethyl)aminomethane hydrochloride (Sigma Chemical Co.) and 8.6 mmol of its base form in 1 L of deionized water and adjusting the pH with HCl or NaOH solution. The 50 mM pH 8.0 TRIS buffer was similarly prepared. All aqueous solutions were prepared using 18 MΩ·cm water (Milli-Q reagent water system, Bedford, MA).

Fabrication of Hydrogel Micropatch Arrays and Microfluidic Devices. Hydrogel arrays and microfluidic devices were fabricated using a slight modification of our previously reported procedure.[3] Briefly, microscope coverslips were functionalized with TPM, which reacts with PEG-DA to ensure adhesion of the hydrogel micropatches to the glass.[17] After PEG-DA was purified using an inhibitor removal kit (Aldrich), it was mixed with 1 wt % of the HMPP initiator and then stored at 4 °C until needed. A three-channel PDMS template mold was placed over a TPM-treated glass slide, and then a photomask having three lines (190-μm lines and 310-μm spaces) was placed on the other side of the glass perpendicular to the PDMS channels (170 μm wide and 24 μm high) (step 1, Scheme 1). Next, a few microliters of the hydrogel precursor solution consisting of 67 vol % PEG-DA in TRIS buffer (pH 7.4) was placed in front of the channel inlets. This solution entered the channels via capillary action. Gel micropatches were formed by exposing the precursor solution to UV light (EFOS Lite E3000, Ontario, Canada) for 2 s. Finally, the PDMS mold was removed (step 2, Scheme 1) and the remaining unpolymerized hydrogel precursor solution was removed by rinsing with water.

Scheme 1

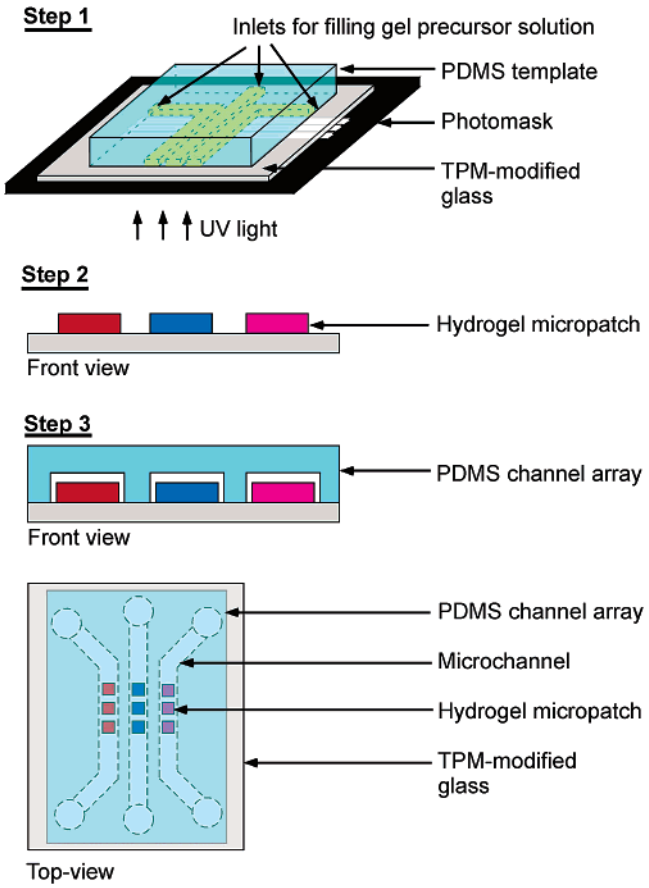

A second PDMS mold having wider and higher channels (270 μm wide and 36 μm high) than the first was used to cover the hydrogel arrays on the glass (step 3, Scheme 1). The larger dimensions of this analysis mold permit fluids to flow around the micropatches. The larger PDMS mold was irreversibly bonded to the micropatch-modified glass slide by exposing both parts to an O_2 plasma (60 W, model PDC-32G, Harrick Scientific, Ossining, NY) and then sealing them together. Alignment of the second mold was carried out manually under an optical microscope. In some experiments a four-channel array was used. For these devices, the template mold was 130 μm wide and 24 μm high, and the analysis mold was 150 μm wide and 36 μm high.

Simultaneous Detection of Different Concentrations of Glucose. GOx (1.0 mg/mL) and HRP (1.0 mg/mL) enzyme stock

(19) Curey, T. E.; Goodey, A.; Tsao, A.; Lavigne, J.; Sohn, Y.; McDevitt, J. T.; Anslyn, E. V.; Neikirk, D.; Shear, J. B. *Anal. Biochem.* **2001**, *293*, 178−184.

solutions were prepared in TRIS buffer (pH 7.4) as follows. First, 10.0 μL of the GOx stock solution and 10.0 μL of the HRP stock solution were mixed with 380.0 μL of TRIS buffer. The GOx/HRP-containing hydrogel precursor solutions were prepared by mixing 25.0 μL of the mixed enzyme solution with 50.0 μL of PEG-DA containing 1 wt % HMPP initiator. This resulted in hydrogel precursor solutions having GOx and HRP concentrations of 8.3 μg/mL.

Enzyme-containing hydrogel micropatch arrays were fabricated within the microfluidic network as described in the previous section. Stock solutions containing 0.500 M glucose were prepared in TRIS buffer solution (pH 7.4), and then these solutions were further diluted with TRIS buffer to prepare lower concentrations. Amplex Red solutions (40 mM) were prepared in anhydrous DMSO and stored at −20 °C. The Amplex Red solutions were thawed just prior to use and then added to the glucose solutions to make the final dye concentration 0.10 mM. Amplex Red photodegrades, so it is important to minimize its exposure to light. Solutions containing Amplex Red and different concentrations of glucose were introduced into each of the channels of a microfluidic device at a flow rate of 1.0 μL/min using a syringe pump (PHD 2000, Harvard Apparatus, Hollistion, MA). Fluorescence micrographs were collected every 30 s for 15 min and then used for quantitative data analysis.

The short-term stability of the GOx/HRP-hydrogel system was examined using four-channel devices fabricated as described earlier. Each channel contained three nominally identical micropatches. On the day of device fabrication, a 5.00 mM glucose solution containing 0.10 mM Amplex Red was introduced into one of the four parallel microchannels, and the average fluorescence signal from the three hydrogel micropatches in the microchannel was used to quantify the stability. The remaining channels were filled with TRIS buffer (pH 7.4) and stored at 4 °C. The activity of the micropatches in these channels was subsequently tested at 2- or 3-day intervals for a week. The average fluorescence signals from these channels were then normalized to the value obtained on the first day of testing. Stability testing was carried out on three independently prepared devices.

Simultaneous Detection of Glucose and Galactose. GOx (1.0 mg/mL), GaOx (1.0 mg/mL), and HRP (1.0 mg/mL) stock solutions were prepared in TRIS buffer (pH 7.4). First, enzyme solutions were prepared using the stock solutions as follows: (1) 10.0 μL of the GOx stock solution and 10.0 μL of the HRP stock solution were mixed in 380.0 μL of TRIS buffer; (2) 80.0 μL of the GaOx stock solution and 10.0 μL of the HRP stock solution were mixed in 310.0 μL of TRIS buffer; (3) 10.0 μL of the HRP stock solution was diluted with 390.0 μL of TRIS buffer. Second, the GOx/HRP-, GaOx/HRP-, and HRP-containing hydrogel precursor solutions were prepared by mixing 25.0 μL of each of the three enzyme solutions with 50.0−μL aliquots of the PEG-DA/initiator solution. Finally, a different set of enzymes was immobilized within each channel of a three-channel microfluidic system.

A solution containing 5.00 mM glucose, 5.00 mM galactose, and 0.10 mM Amplex Red in TRIS buffer (pH 7.4) was pumped into the three channels at 1.0 μL/min. Fluorescence micrographs were collected every 30 s for 15 min. After rinsing the channels with TRIS buffer for 15 min at 1.0 μL/min, a second solution containing only 5.00 mM glucose and 0.10 mM Amplex Red was tested. Finally, after rinsing the channels again, a third solution containing only 5.00 mM galactose and 0.10 mM Amplex Red solution was tested.

Acetylcholine Analysis and Paraoxon Sensing. AChE (1.0 mg/mL), ChOx (7.7 mg/mL), and HRP (0.1 mg/mL) enzyme stock solutions were prepared in 50.0 mM TRIS buffer (pH 8.0). The enzyme stock solutions were divided into 100-μL aliquots and then stored at −20 °C until needed. Hydrogel precursor solutions containing enzymes were prepared as follows: (1) 15.0 μL of the AChE stock solution, 15.0 μL of the ChOx stock solution, and 20.0 μL of the HRP stock solution were mixed with 100.0 μL of the PEG-DA/initiator stock solution; (2) 15.0 μL of the ChOx stock solution, 20.0 μL of the HRP stock solution, and 15.0 μL of TRIS buffer were mixed with 100.0 μL of the PEG-DA/initiator stock solution; (3) 15.0 μL of the AChE stock solution, 20.0 μL of the HRP stock solution, and 15.0 μL of TRIS buffer were mixed with 100.0 μL of the PEG-DA/initiator stock solution; (4) 15.0 μL of the AChE stock solution, 15.0 μL of the ChOx stock solution, and 20.0 μL of TRIS buffer were mixed with 100.0 μL of the PEG-DA/initiator stock solution. Micropatches were prepared using these solutions, and then the devices were fabricated as described earlier.

Analyte solutions were prepared as follows. Acetylcholine powder contained in small vials was purchased and stored at −20 °C until needed. 20.0 mM acetylcholine solutions containing 0.10 mM Amplex Red were prepared in TRIS buffer (pH 8.0) just before use. Paraoxon was purified using a literature procedure,[20] and then a paraoxon stock solution (0.80 mM) was prepared in water and stored at 4 °C until needed. Different concentrations of paraoxon solutions were pumped into the channels containing composite AChE/ChOx/HRP-entrapped hydrogel micropatches at 0.1 μL/min for 20 min. After rinsing the channels with deionized water at 1.0 μL/min for 10 min, the mixed solution of acetylcholine and Amplex Red was pumped into the four channels and fluorescence micrographs were collected every 30 s for 15 min.

Analysis. All micrographs were collected using an inverted optical/epifluroescence microscope (Nikon Eclipse TE 300, Nikon Co., Tokyo, Japan) equipped with a cube-type XF-102-2 filter set (Omega Optical, Inc., Brattleboro, VT). The images were obtained with either a 24-bit color CCD camera (D1H, Nikon Co.) or a 16-bit gray scale CCD camera (Photometrics Ltd., Tucson, AZ). Images were captured every 30 s for 15 min. The CCD signal was integrated for 0.7 s. To minimize photobleaching, the microdevices were only illuminated during data acquisition. The images were analyzed using V++ software (Digital Optics, Auckland, New Zealand), which provides the average fluorescence signal from a selected area of pixels in the fluorescence micrograph.

RESULTS AND DISCUSSION

Fabrication of Hydrogel Micropatch Arrays and Microfluidic Devices. Figure 1a is an optical micrograph showing a photomask and an array of three PDMS channels (oriented vertically) before filling with the hydrogel precursor solution. The hydrogel micropatches shown in Figure 1b result from filling the channels with the hydrogel precursor solution, photopolymerizing

(20) Omburo, G. A.; Kuo, J. M.; Mullins, L. S.; Raushel, F. M. *J. Biol. Chem.* **1992**, *267*, 13278−13283.

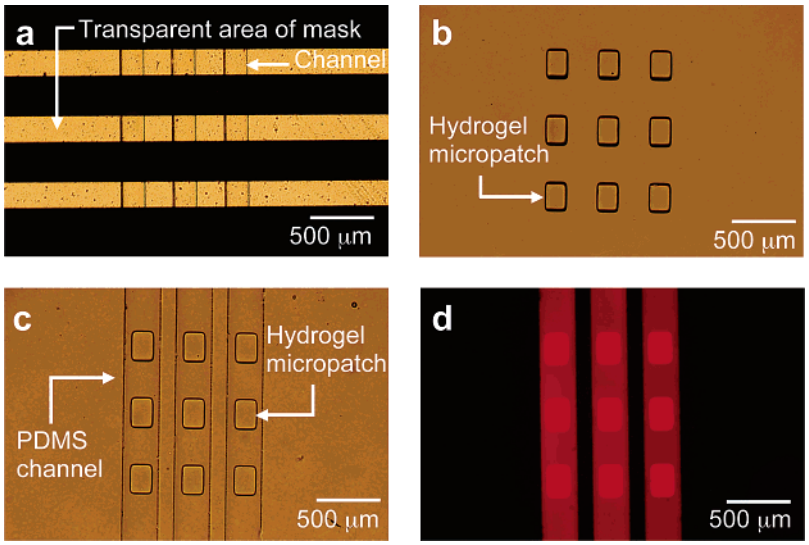

Figure 1. (a) Optical micrograph showing a photomask and an array of three PDMS channels before filling with hydrogel precursor solution (step 1, Scheme 1). (b) Optical micrograph of an array of hydrogel micropatches confined to the surface of TPM-modified glass (step 2, Scheme 1). (c) Optical micrograph of a completed microfluidic device (step 3, Scheme 1). (d) Fluorescence micrograph of the microfluidic device shown in (c) after exposure to the fluorescent dye resorufin. All micrographs were obtained with a Nikon 24-bit CCD camera.

it through the mask, removing the PDMS template, and then removing unpolymerized precursor solution by rinsing (step 2, Scheme 1). Micropatches having dimensions as small as 50 μm could be prepared by this method, but the width and length of the micropatches shown in Figure 1b (160 $\pm$ 5 and 240 $\pm$ 7 μm, respectively) are typical of those used throughout this work. The difference between the width of the mask (190 μm) and length of the micropatches (240 μm) is likely a consequence of either diffusion of photoradicals beyond the illuminated region of the mask[17] or light scattering within the fluidic system. The height of the micropatches is defined by the height of the PDMS template ($\sim$24 μm).

Device fabrication was completed by bonding a PDMS channel array having larger dimensions (270 μm wide and 36 μm high) than the template to the glass slide supporting the micropatches (step 3, Scheme 1 and Figure 1c). This results in open-channel regions above and to the side of the micropatches that permit analyte solutions to flow through the channel. Figure 1d is a fluorescence micrograph obtained after flowing a solution containing the dye resorufin through the three channels. Resorufin selectively sorbs into the relatively hydrophobic micropatches (dark red squares in Figure 1d), demonstrating that small molecules are easily able to penetrate into the nanoporous network of the hydrogel. No fluorescence was detected between the three channels, indicating that the fabrication procedure results in a robust seal between the PDMS channel assembly and the TPM-modified glass surface.

Simultaneous Detection of Different Concentrations of Glucose. To demonstrate that arrays of hydrogel micropatches containing enzymes can be used to simultaneously detect different concentrations of the same analyte, we prepared a microfluidic device in which each micropatch contained GOx and HRP. In this case, all 12 micropatches were nominally identical in composition and only the analyte concentration in the flow stream varied. The width and length of the hydrogel micropatches shown in Figure 2a are 130 $\pm$ 5 and 253 $\pm$ 5 μm, respectively. Scheme 2 shows the consecutive enzyme-catalyzed reactions that occur within each micropatch in the presence of a solution containing both glucose and Amplex Red, and Scheme 3 is a side view of an individual channel showing the transport and reaction processes that occur during analysis. Briefly, a solution containing glucose (**1**) and Amplex Red (**4**) is continuously supplied to the micropatches by a syringe pump via the channels. After diffusing (A in Scheme 3) into the micropatch, glucose encounters the entrapped GOx and is converted into gluconolactone (**2**) and H_2O_2 (**3**). Next, non-fluorescent Amplex Red reacts with H_2O_2 in the presence of HRP to produce strongly fluorescent resorufin (**5**) (B in Scheme 3). Some of the resorufin remains within the micropatch, and the remainder diffuses out of the hydrogel (C in Scheme 3) and into the solution flowing through the channels. When the transport of glucose and resorufin in to and out of the micropatch, respectively, are balanced, then the magnitude of fluorescence from the micropatches should achieve steady state. In principle, there should be a relationship between the concentration of glucose introduced into the channel and the intensity of the resulting fluorescence.

To test this latter hypothesis, buffer solutions containing 0.10 mM Amplex Red plus 0, 1.00, 3.00, or 5.00 mM glucose were simultaneously introduced into each of the four channels at a flow rate of 1.0 μL/min. Fluorescence micrographs were obtained every 30 s for 15 min under flowing conditions. Figure 2a is a typical fluorescence micrograph obtained 15 min after glucose was first introduced into the channels. Time-dependent fluorescence intensity profiles were extracted for each micropatch using micrographs such as this. Figure 2b shows these data for the hydrogel micropatches in the top row of Figure 2a. Data for the other two micropatches in each channel were also obtained. The net fluorescence intensity was calculated by subtracting the intensity of the micropatch in channel 1 (no glucose present) from the fluorescence intensities arising from the micropatches in channels 2–4. The results show that the fluorescence intensity from all the micropatches reach steady state within 5 min. Accordingly, the 10 data points between 10 and 15 min in each curve of Figure 2b were averaged. This value was then averaged with the

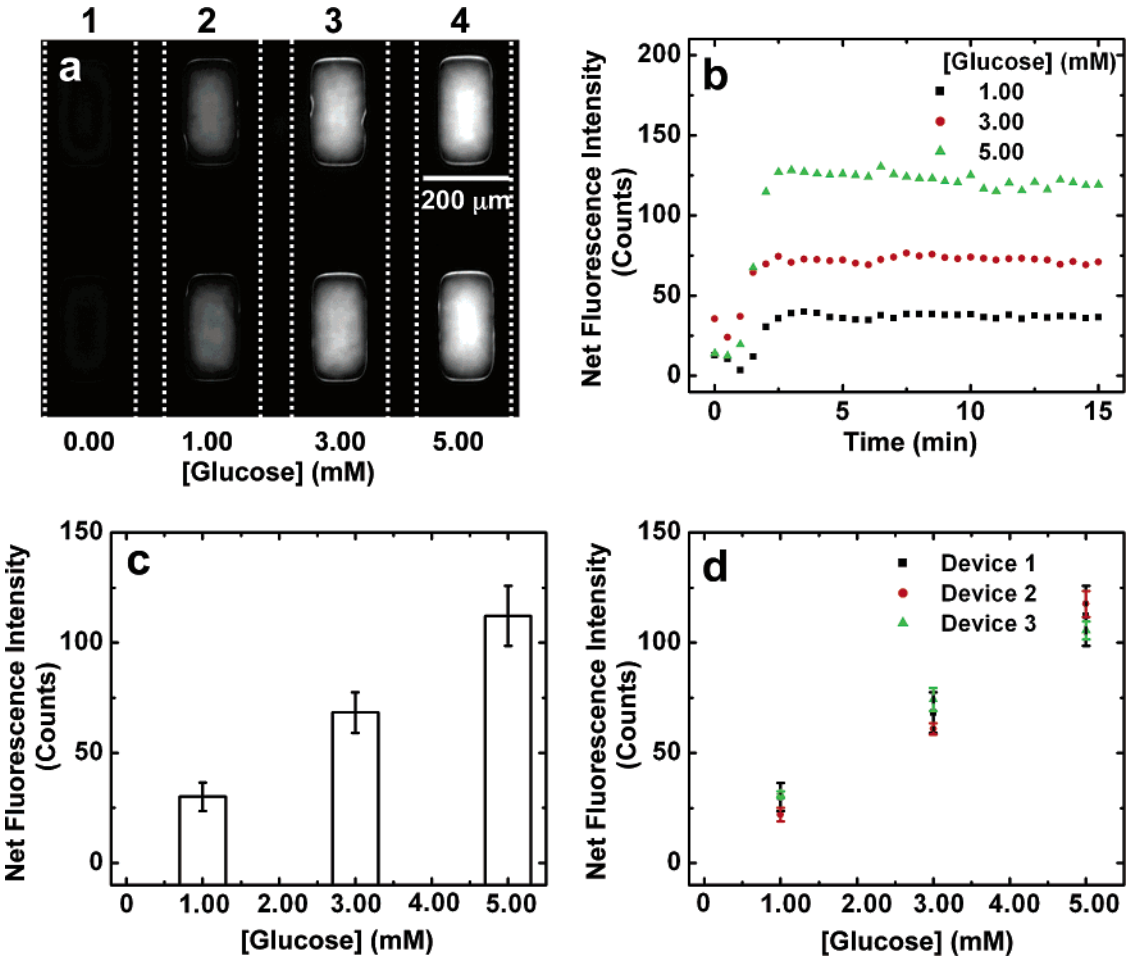

Figure 2. (a) Fluorescence micrograph obtained 15 min after solutions containing 0.10 mM Amplex Red plus different concentrations of glucose (shown at the bottom of each channel) were introduced into each of the four channels. The flow rate was 1.0 μL/min. Each micropatch contained both GOx and HRP. The fluorescence emission was integrated for 0.7 s. The dashed white lines indicate the positions of channel walls. (b) Time-dependent net fluorescence intensity profiles collected from the hydrogel micropatches shown in the top row of (a). The net fluorescence intensity was obtained by subtracting the intensity of the micropatch in channel 1 (no glucose present) from the fluorescence intensities arising from the micropatches in channels 2−4. (c) Graph showing the average net fluorescence intensity as a function of the glucose concentration for the three micropatches present in each channel of the device shown in (a). The error bars represent 1σ for the three micropatches. (d) Plot of net fluorescence intensity as a function of glucose concentration for three independently prepared microfluidic devices. The error bars represent 1σ for the three micropatches in each channel of each device. Fluorescence micrographs were obtained with a Photometrics 16-bit gray scale CCD camera.

Scheme 2

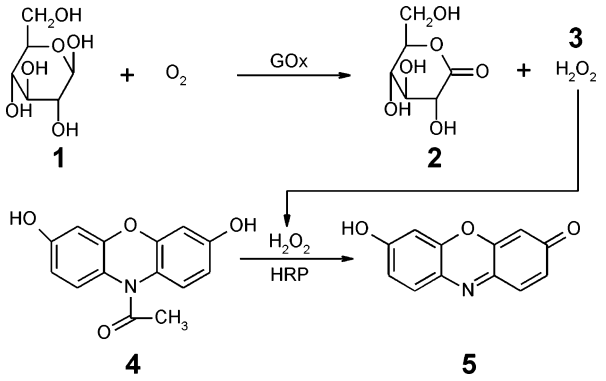

Scheme 3

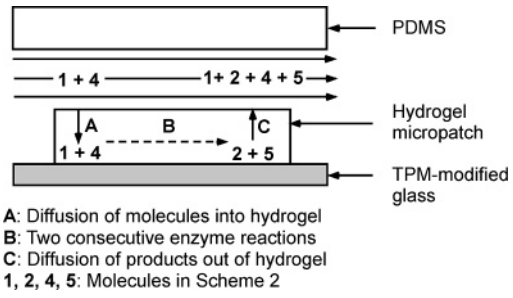

corresponding values for the other two micropatches in each channel. These averages are displayed in Figure 2c, where the error bars represent the standard deviations of the values obtained from the three hydrogel micropatches within the same channel. Data were then obtained from two additional, independently prepared microdevices, and the resulting average net fluorescence intensity from all three devices is plotted as a function of glucose concentration in Figure 2d. Here the error bars represent the standard deviations of the three values obtained from the three hydrogel micropatches within the same channel. The key result is that there is a linear correspondence between the net steady-state fluorescence intensity and the glucose concentration over the physiologically important range of 1.00−5.00 mM (detection

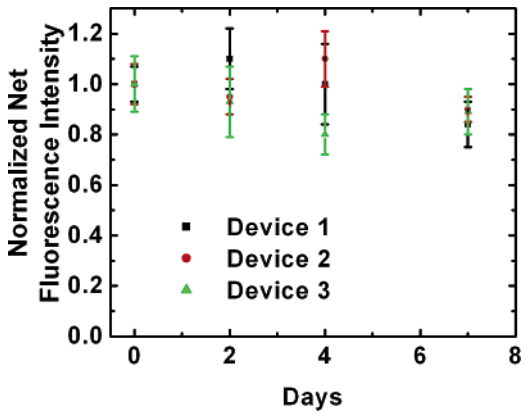

Figure 3. Short-term stability test of the activity of GOx and HRP coimmobilized within hydrogel micropatches using three independently prepared microfluidic devices.

limit, 0.8 ± 0.4 mM). Because additional channels could easily be added to the array, it would be possible to simultaneously compare the fluorescence of standard glucose solutions to real samples, thereby providing quantitation. This microfluidic glucose analysis can be carried out within 15 min and consumes ~15 μL of sample/channel.

There are three main advantages of this microfluidic assay compared to equivalent assays carried out using microtiter plates. First, the microfluidic approach relies on a steady-state flow of the analyte. This eliminates the need for pipetting and mixing of very small volumes. Additionally, solvent evaporation, which is often encountered when using microtiter wells,[21] is negligible in microfluidic channels. Second, additional sample preparation steps could be added to a fully integrated microfluidic system. For blood samples, this might include direct coupling of a microdialysis step to the microfluidic chip.[22] Third, the analysis is performed using on-chip standards, which eliminates the need for absolute calibration.

In principle, the sensitivity and limit of detection (LOD) of this type of sensor could be improved by increasing the concentration of enzymes within the hydrogel. However, at high enzyme concentrations, we observed nonuniform fluorescence emission from individual micropatches, which we attribute to enzyme aggregation. For example, micropatches prepared from hydrogel precursor solutions containing >50 μg/mL HRP exhibited multiple bright spots (Supporting Information, Figure S1), while those prepared from solutions having GOx and HRP concentrations of <16 μg/mL appeared homogeneous (Figure 2a). Hydrogels containing aggregated enzymes resulted in poor measurement reproducibility. We found that HRP (and not GOx) was primarily responsible for enzyme aggregation (Supporting Information, Figures S2 and S3).

Figure 3 shows the short-term stability of hydrogel-entrapped GOx/HRP. The data indicate that the enzymes exhibit only a slight loss in activity when they are stored in buffer at 4 °C. These data also indicate that the enzymes do not leach out of the hydrogel micropatches. If they did, then a decrease in fluorescence intensity would be observed.

(21) Babiak, P.; Reymond, J.-L. *Anal. Chem.* **2005**, *77*, 373−377.
(22) Kurita, R.; Hayashi, K.; Fan, X.; Yamamoto, K.; Kato, T.; Niwa, O. *Sens. Actuators, B* **2002**, 296−303.

Scheme 4

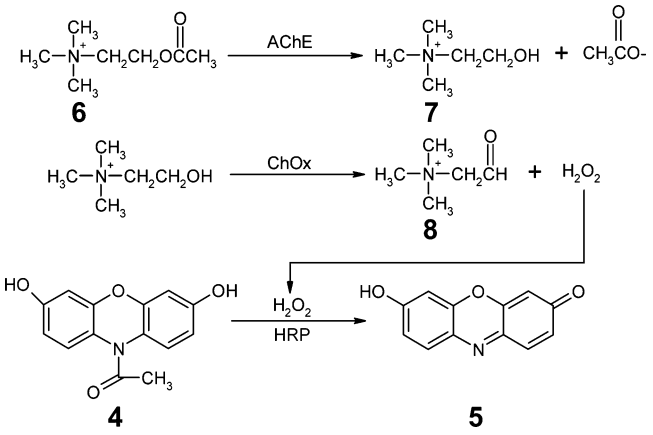

Simultaneous Detection of Glucose and Galactose. Here we show that two closely related substrates, glucose and galactose, can be detected using hydrogel-entrapped enzymes. In contrast to the results presented in the previous section, the micropatches for the present experiments were configured with different enzymes. Specifically, as shown in Figure 4a, the micropatches in channels 1−3 contained GOx + HRP, HRP only, and GaOx + HRP, respectively. In this experiment, a buffer solution containing 5.00 mM each of glucose and galactose plus 0.10 mM Amplex Red was introduced into the three channels shown in Figure 4a for 15 min, and fluorescence micrographs were obtained every 30 s. The micropatches in channels 1 (GOx + HRP) and 3 (GaOx + HRP) react with their respective substrates, and resorufin fluorescence is observed. However, no fluorescence is detected in the absence of the enzyme required to generate H_2O_2 (channel 2). An experiment designed to determine the extent of cross-reactivity between glucose and the GaOx-entrapped micropatch, and galactose and the GOx-entrapped micropatch, is shown in Figure 4b. Here, a 5.00 mM glucose solution containing 0.10 mM Amplex Red was passed through all three channels for 15 min. The analogous experiment for galactose is shown in Figure 4c. Qualitatively, the data indicate no cross-reactivity.

A quantitative representation of the micrographs in Figure 4a−c is shown in Figure 4d. The net fluorescence intensity of individual micropatches was obtained by subtracting the fluorescence intensity of the micropatch in channel 2 (HRP only) shown in Figure 4a−c from the fluorescence intensities of the micropatches in channels 1 (GOx + HRP) and 3 (GaOx + HRP) in Figure 4a−c. There are three key observations that arise from Figure 4. First, the magnitude of the net fluorescence intensity resulting from the presence of glucose and galactose is the same regardless of whether the analyte is present alone or in a mixture. Second, the fluorescence intensity for a particular target analyte is substantially higher in the presence of its corresponding enzyme than when that enzyme is absent. Third, the fluorescence intensity observed for galactose is only 40% of that measured for glucose. Considering that the GaOx concentration used to prepare the micropatches in channel 3 was 8 times higher than for the corresponding glucose micropatches, we conclude that GaOx micropatches are 20 times less efficient at generating H_2O_2 compared to the GOx micropatches. The activity of the two enzymes was measured in bulk solution using a conventional spectrofluorometer, and the activity per unit weight of GOx was

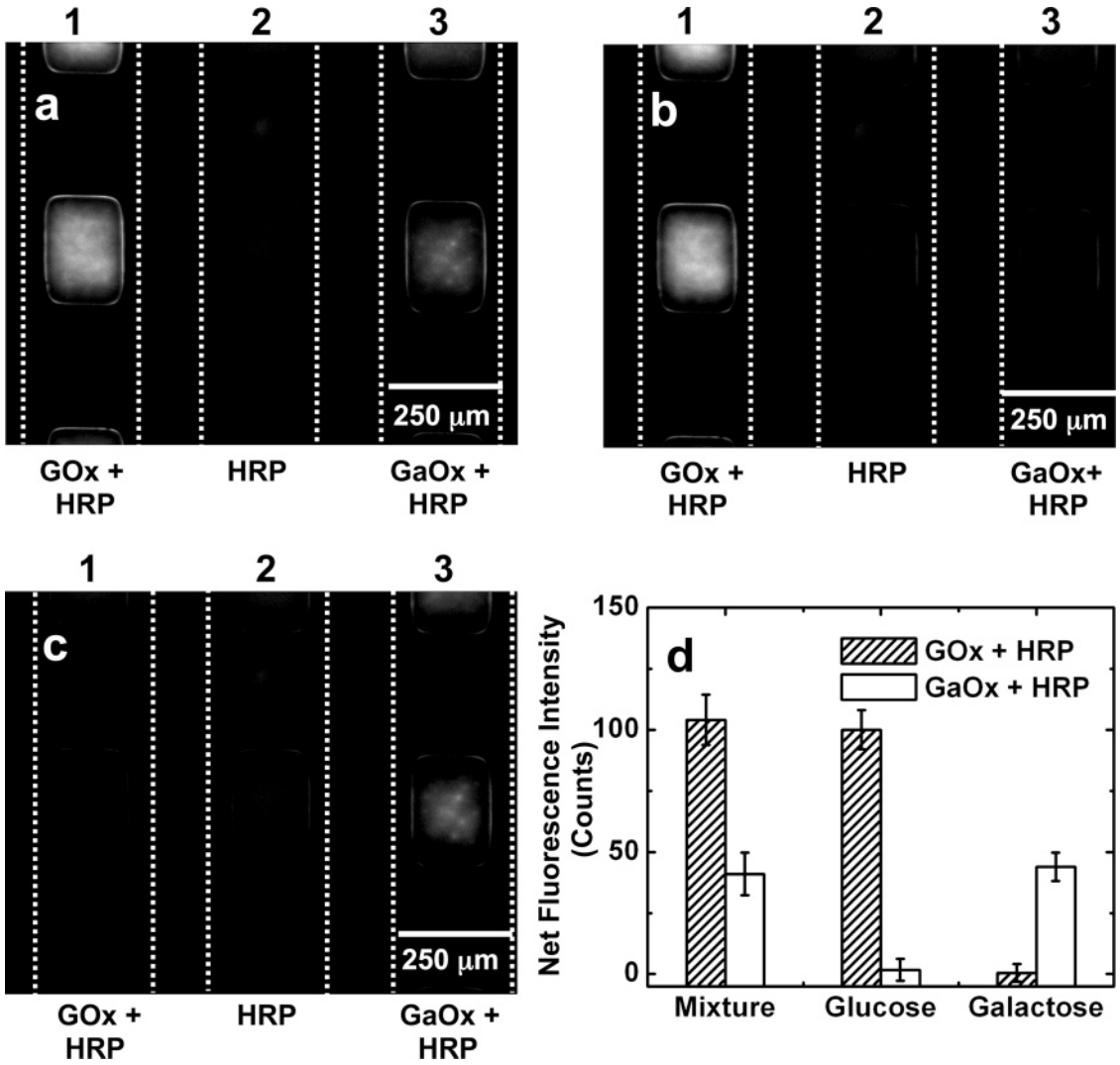

Figure 4. (a) Fluorescence micrograph showing an array of hydrogel micropatches entrapping the enzymes shown at the bottom of each channel. The data were obtained 15 min after a solution containing 5.00 mM glucose, 5.00 mM galactose, and 0.10 mM Amplex Red was introduced into each of the three channels. (b) Fluorescence micrograph showing an array of hydrogel micropatches entrapping the enzymes shown at the bottom of each channel. The data were obtained 15 min after a solution containing 5.00 mM glucose and 0.10 mM Amplex Red was introduced into each of the three channels. (c) Fluorescence micrograph showing an array of hydrogel micropatches entrapping the enzymes shown at the bottom of each channel. The data were obtained 15 min after a solution containing 5.00 mM galactose and 0.10 mM Amplex Red was introduced into each of the three channels. In all cases the flow rate was 1.0 μL/min. (d) The average net fluorescence intensity for the three micropatches contained within channels 1 and 3 in (a)−(c). The net fluorescence intensity was obtained by subtracting the fluorescence intensity of the hydrogel micropatch in channel 2 from the fluorescence intensities of the hydrogel micropatches in channels 1 and 3. The error bars represent 1σ for the three micropatches in the individual channels. The fluorescence signal was integrated for 0.7 s. Fluorescence micrographs were obtained with a Photometrics CCD camera.

found to be only 3.3 times that of GaOx. This means that the activity of GaOx is suppressed by a factor of ~6 when it is incorporated into the hydrogel matrix. The effect of different matrixes on enzyme activity has been observed previously, so this result is not surprising.[23]

Acetylcholine Analysis and Paraoxon Sensing. AChE is an enzyme that converts the neurotransmitter acetylcholine (**6**, Scheme 4) to choline (**7**). Many organophosphates inhibit the activity of AChE and thereby disrupt the nervous systems of animals.[24] Accordingly, AChE is frequently used as an active component in biosensors designed to detect pesticides and chemical weapons.[25−36] Here, we show that an appropriately configured array of hydrogel-entrapped enzymes can be used to detect organophosphate inhibitors. Specifically, the activity of

(23) Bickerstaff, G. F., Ed. *Immobilization of enzymes and cells*; Humana Press: Totowa, NJ, 1997.
(24) Fukuto, T. R. *Environ. Health Perspect.* **1990**, *87*, 245−254.
(25) Alfthan, K.; Kenttanmaa, H.; Zukale, T. *Anal. Chim. Acta* **1989**, *217*, 43−51.
(26) Tran-Minh, C.; Pandey, P. C.; Kumaran, S. *Biosens. Bioelectron*. **1990**, *5*, 461−471.
(27) Leon-Gonzalez, M. E.; Townshend, A. *Anal. Chim. Acta* **1990**, *236*, 267−272.
(28) Moris, P. M.; Alexandre, I.; Roger, M.; Remacle, J. *Anal. Chim. Acta* **1995**, *302*, 53−59.
(29) Hadd, A. G.; Jacobson, S. C.; Ramsey, J. M. *Anal. Chem.* **1999**, *71*, 5206−5212.
(30) Singh, A. K.; Flounders, A. W.; Volponi, J. V.; Ashley, C. S.; Wally, K.; Schoeniger, J. S. *Biosens. Bioelectron.* **1999**, *14*, 703−713.
(31) Doong, R.-A.; Tsai, H.-C. *Anal. Chim. Acta* **2001**, *434*, 239−246.

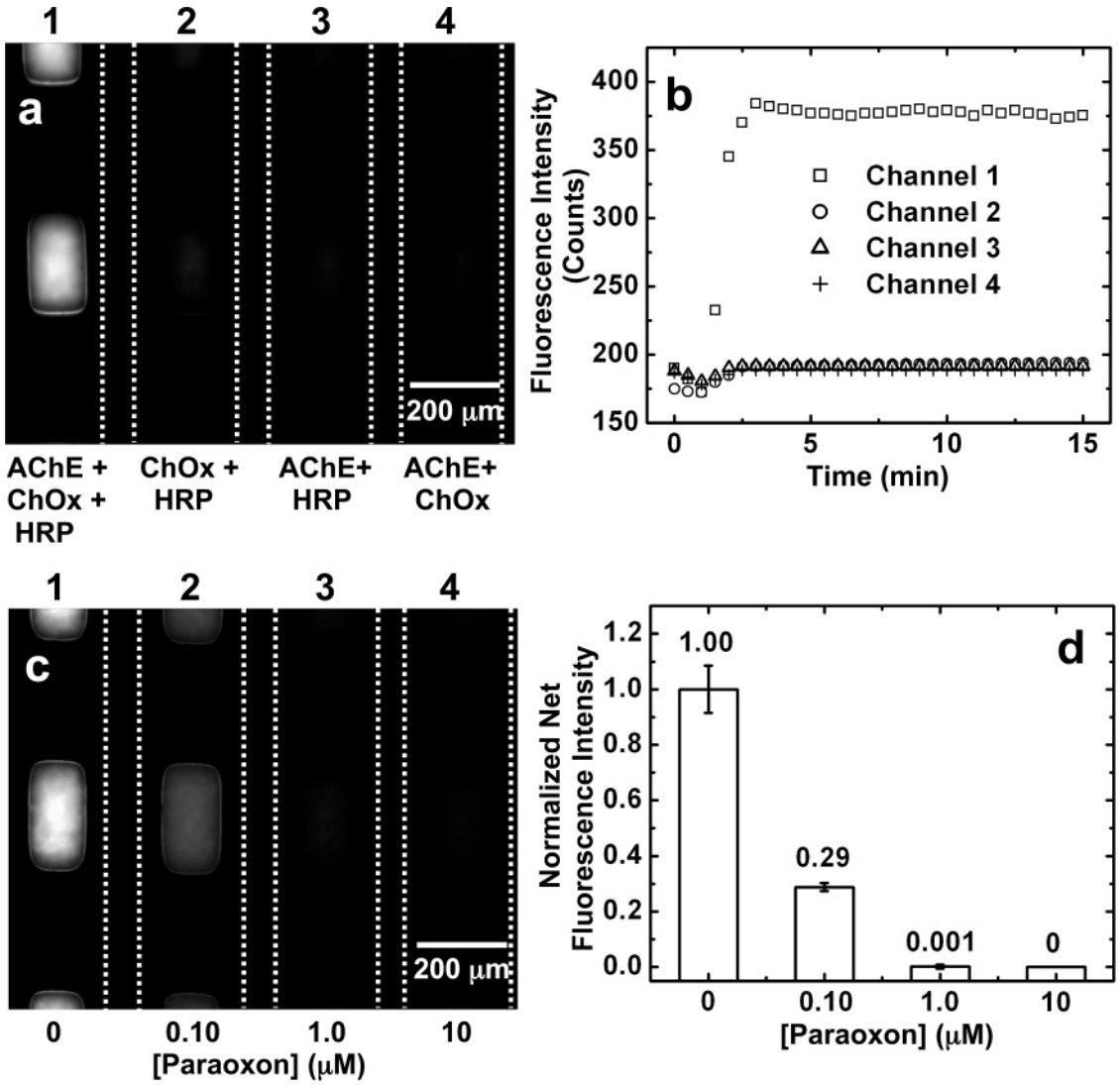

Figure 5. (a) Fluorescence micrograph of an array of hydrogel micropatches containing the enzyme combinations shown below each channel. The data were obtained 15 min after 20.0 mM acetylcholine plus 0.10 mM Amplex Red was introduced into each of the four channels at 1.0 μL/min. (b) Time-dependent fluorescence intensity profiles collected from the hydrogel micropatches in the center of the micrograph shown in (a). The fluorescence intensity was not background subtracted. (c) Fluorescence micrograph showing the effect of paraoxon concentration on the fluorescence intensity of hydrogel micropatches. Each hydrogel micropatch contained AChE, ChOx, and HRP. The micropatches were exposed to flowing (0.1 μL/min) paraoxon at the concentrations indicated below each channel for 20 min, rinsed with water for 10 min, and then the fluorescence micrograph was obtained 15 min after 20.0 mM acetylcholine plus 0.10 mM Amplex Red in TRIS buffer (pH 8.0) was introduced into each of the four channels at 1.0 μL/min. (d) The average normalized net fluorescence intensity obtained from the fluorescence micrograph shown in (c). The error bars represent 1σ for the three micropatches in the individual channels. All the fluorescence signals were integrated for 0.7 s. Fluorescence micrographs were obtained with a Photometrics CCD camera.

AChE can be probed by coupling it to ChOx and HRP. As shown in Scheme 4, a mixed solution of acetylcholine and Amplex Red ultimately produces fluorescent resorufin in the presence of AChE, ChOx, and HRP.[37,38]

The first step in this part of the study was to ensure that the reactions shown in Scheme 4 would proceed within a hydrogel micropatch. Accordingly, micropatches were configured with four different combinations of entrapped enzymes (AChE + ChOx + HRP, ChOx + HRP, AChE + HRP, AChE + ChOx) as shown at the bottom of Figure 5a, and then a 20.0 mM acetylcholine solution containing 0.10 mM Amplex Red was pumped into all four channels. The results clearly indicate that if just one of the enzymes in the reaction pathway (Scheme 4) is absent, then no fluorescence is observed. Figure 5b is a quantitative representation of the time evolution of the fluorescence arising from the micropatches shown in Figure 5a.

Next, we examined the effect of an organophosphate inhibitor, paraoxon, on the fluorescence intensity of micropatches containing

(32) Kok, F. N.; Bozoglu, F.; Hasirci, V. *Biosens. Bioelectron.* **2002**, *17*, 531−539.
(33) Walker, J. P.; Asher, S. A. *Anal. Chem.* **2005**, *77*, 1596−1600.
(34) Skladal, P. *Anal. Chim. Acta* **1992**, *269*, 281−287.
(35) La Rosa, C.; Pariente, F.; Hernández, L.; Lorenzo, E. *Anal. Chim. Acta* **1994**, *295*, 273−282.
(36) Campanella, L.; De Luca, S.; Sammartino, M. P.; Tomassetti, M. *Anal. Chim. Acta* **1999**, *385*, 59−71.
(37) Haugland, R. P. *Handbook of fluorescent probes and research chemicals*, 6th ed.; Molecular Probes, Inc.: Eugene, OR, 1996; pp 552−556.
(38) Zhou, M.; Diwu, Z.; Panchuk-Voloshina, N.; Haugland, R. P. *Anal. Biochem.* **1997**, *253*, 162−168.

AChE, ChOx, and HRP. As suggested by Scheme 4, inhibition of AChE will reduce the concentration of H_2O_2 in the micropatch, and this in turn will reduce the concentration of fluorescent resorufin. Figures 5c shows the effect of flowing (0.1 μL/min for 20 min) different paraoxon concentrations (0, 0.10, 1.0, and 10 μM in channels 1, 2, 3, and 4, respectively) on the fluorescence intensity of the micropatches. The micrographs were obtained after exposing the micropatches to paraoxon, rinsing the channels with water for 10 min, and then introducing pH 8.0 TRIS buffer containing acetylcholine (20.0 mM) and Amplex Red (0.10 mM). The results indicate that resorufin fluorescence is attenuated as the paraoxon concentration increases.

A quantitative representation of the data in Figure 5c is provided in Figure 5d. A paraoxon concentration of 10 μM completely inhibits AChE, so the fluorescence of the micropatch in channel 4 (Figure 5c) was subtracted from the fluorescence in the other micropatches to yield the normalized net fluorescence plotted in Figure 5d as a function of paraoxon concentration. The data indicate that when the hydrogel-entrapped enzymes was exposed to 0.10 μM paraoxon for 20 min, the AChE activity was reduced by ~70%, while at paraoxon concentrations exceeding 1.0 μM fluorescence was completely inhibited.

The lowest LOD limit for organophosphate sensors that rely on AChE is in the femtomolar range.[33] AChE-based assays employing amperometric[34−36] and potentiometric[26] detection have limits of detection in the picomolar to nanomolar range. Spectrophotometric,[27] chemiluminescent,[28] and fluorometric[31] assays have LODs in the nanomolar range. However, from a practical point of view, LODs are probably less important than the development of portable, robust, low-cost organophosphate biosensors. Although there remain some experimental conditions to optimize in the system reported here, the data suggest an LOD well below 100 nM.

We examined the short-term stability of the hydrogel-entrapped AChE/ChOx/HRP enzymes using the approach described earlier for micropatches containing GOx and HRP. The data indicate that storage at 4 °C in buffer does not result in a significant loss of enzyme activity over a period of 8 days (Supporting Information, Figure S4).

(39) Zhan, W.; Alvarez, J.; Crooks, R. M. *J. Am. Chem. Soc.* **2002**, *124*, 13265−13270.

SUMMARY AND CONCLUSIONS

We have demonstrated that a microfluidic sensor based on an array of hydrogel-entrapped enzymes can be used to simultaneously detect different concentrations of the same analyte (glucose) or multiple analytes (glucose and galactose) in real time. Furthermore, the concentration of paraoxon, an AChE inhibitor, can be quantified using the same basic approach. The hydrogel micropatch arrays and the microfluidic systems are straightforward to fabricate, and the hydrogels provide a convenient, biocompatible matrix for the enzymes. Isolation of the micropatches within different microfluidic channels eliminates the possibility of cross-talk between enzymes.

The hydrogel array approach described here could be extended to other assays that require simultaneous measurement of multiple analytes by incorporating appropriate receptor molecules within the hydrogel matrix. Finally, in addition to optical detection methods, this same general approach could be used with electrochemical detection, which would reduce cost and simplify the system.[39]

ACKNOWLEDGMENT

Financial support from the Texas Institute for Intelligent Bio-Nano Materials and Structures for Aerospace Vehicles, funded by NASA Cooperative Agreement NCC-1-02038, and from the U.S. Army Medical Research & Materiel Command is gratefully acknowledged. We also thank for the TAMU Materials Characterization Facility for providing the microfabrication facilities necessary for this work. We are grateful to Dr. Gi Hun Seong and Dr. Wei Zhan for helpful discussions and assistance with fabrication of microfluidic devices.

SUPPORTING INFORMATION AVAILABLE

Fluorescence micrographs showing enzyme aggregation as a function of GOx and HRP concentrations, fluorescence and optical micrographs confirming that the enzyme aggregates within hydrogel micropatches mainly resulted from HRP, and results of a short-term stability test of micropatches containing AChE, ChOx, and HRP. This material is available free of charge via the Internet at http://pubs.acs.org.

Received for review May 8, 2005. Accepted August 19, 2005.

AC0507993